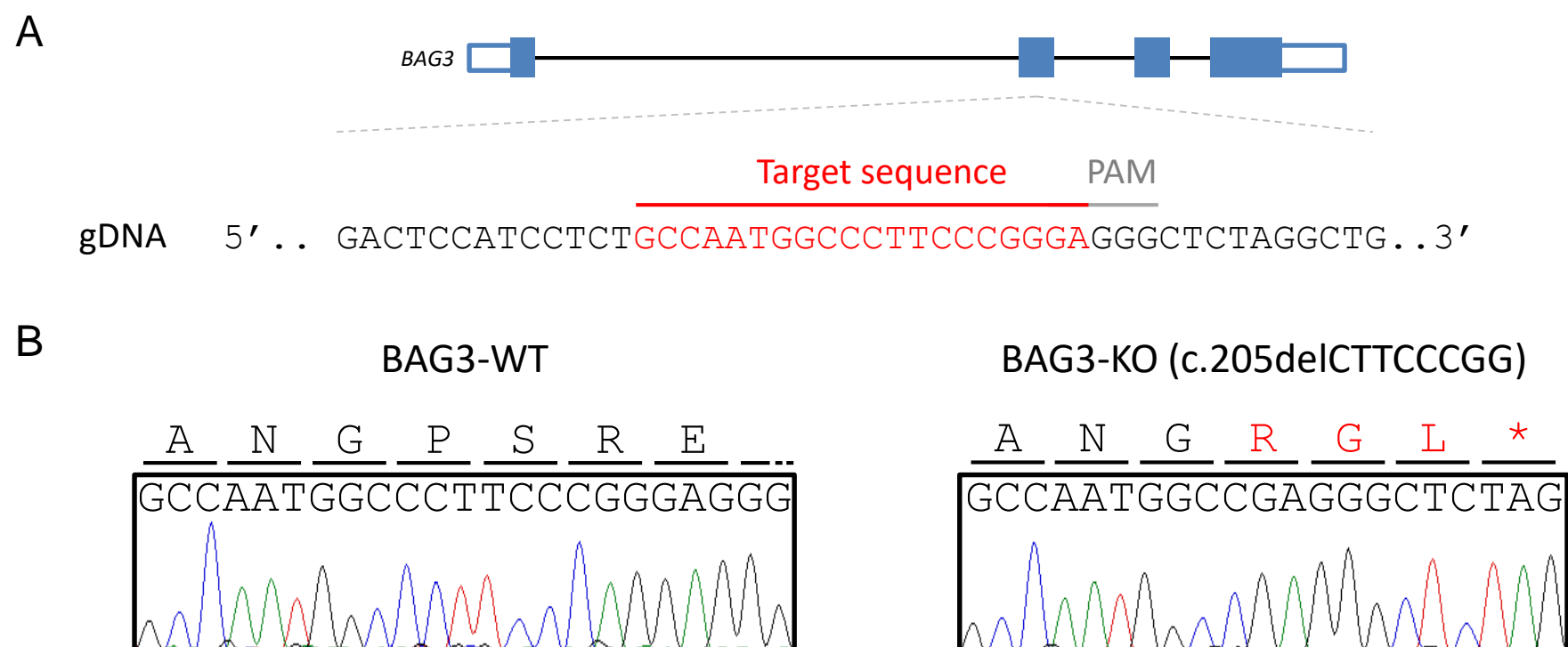
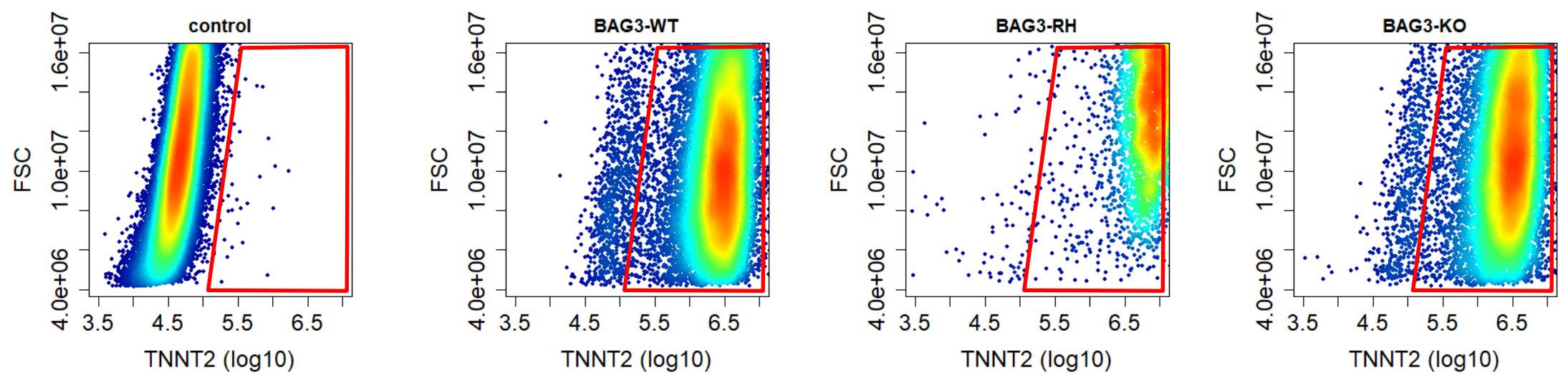


Supplementary Figure 1



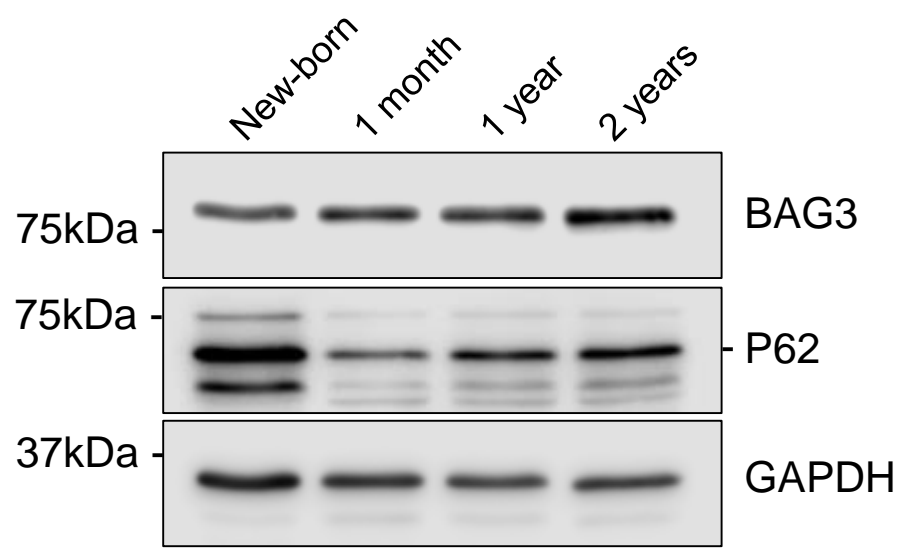
Supplementary Figure 1: BAG3 knockout (KO) in iPSC-CMs. (A) Schema of *BAG3* gene indicating target (red) and PAM (grey) sequence against which an sgRNA was designed. (B) Sanger sequence traces and corresponding amino acid sequences of an unedited clone (*BAG3*-WT, left) and a clone harboring a homozygous 8bp deletion and premature stop codon (*BAG3*-KO (c.205delCTTCCCGG), right). Mutated amino acids are shown in red and * denotes a premature stop codon.

Supplementary Figure 2

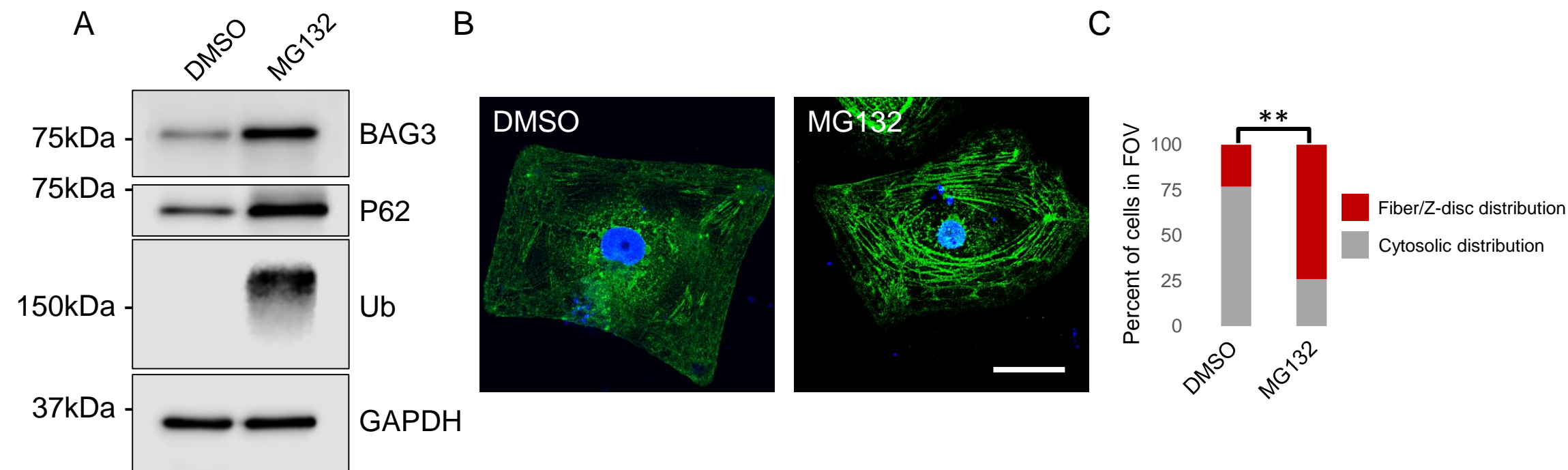


Supplementary Figure 2: Confirmation of iPSC-derived cardiomyocyte formation using flow cytometry-based measurement of cardiac Troponin expression. Representative scatter plots showing cardiac Troponin expression (x axis) and forward scatter (y axis) in control iPSC-CMs (secondary antibody only), BAG3-WT iPSC-CMs, BAG3-RH iPSC-CMs and BAG3-KO iPSC-CMs. Each point represents a cell and only live, singlets, selected based on gating using forward- and side-scatter measurements (not shown) were analyzed and are displayed. From left to right, gated areas contains <1%, 90%, 92% and 93% of the total cell populations, respectively.

Supplementary Figure 3

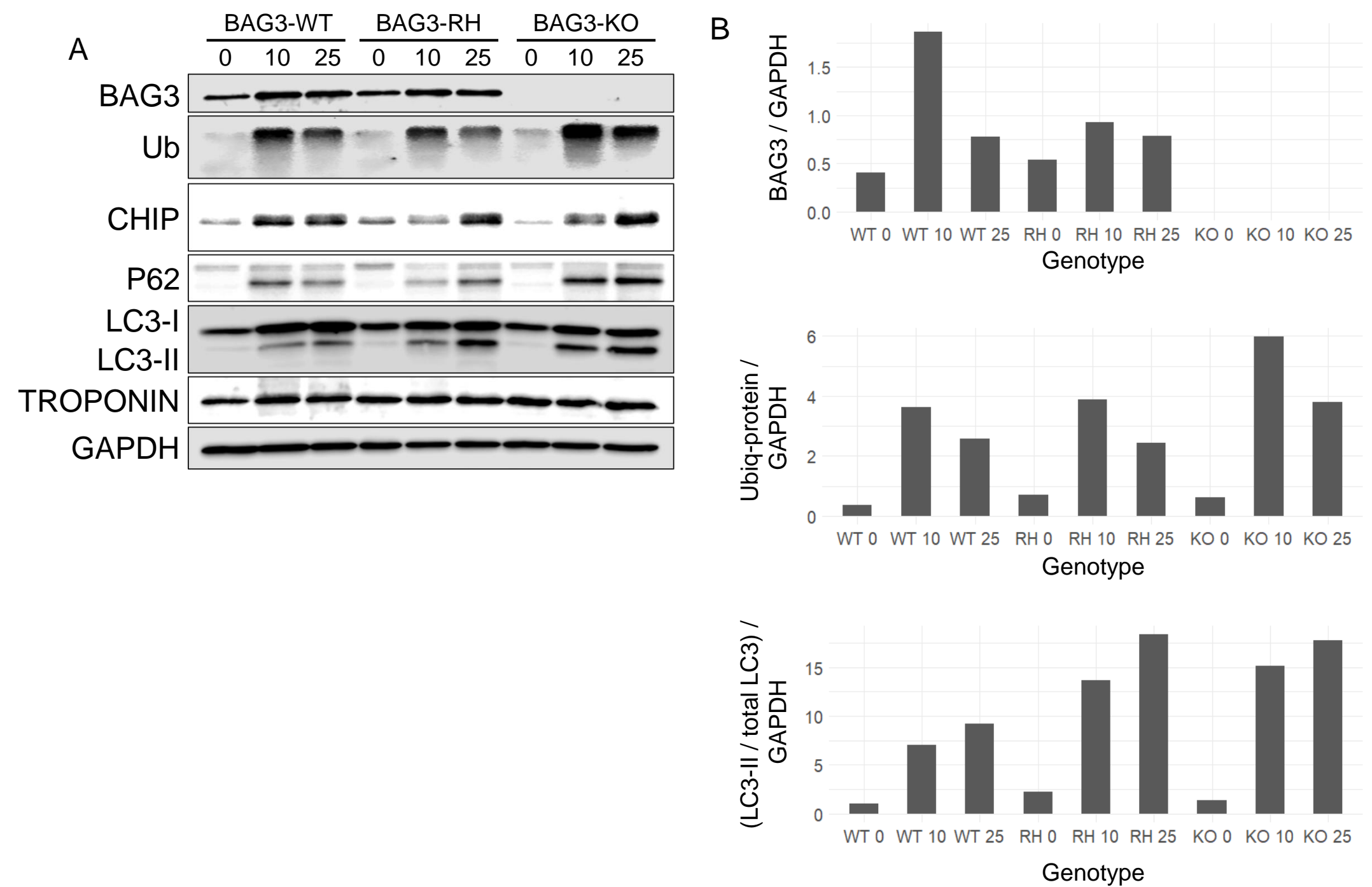


Supplementary Figure 3: BAG3 and P62 protein expression in mouse heart during ageing. Expression of both BAG3 and P62 increases with ageing. Note highest P62 expression in newborn heart, reflective of starvation-induced macroautophagy triggered immediately following birth.

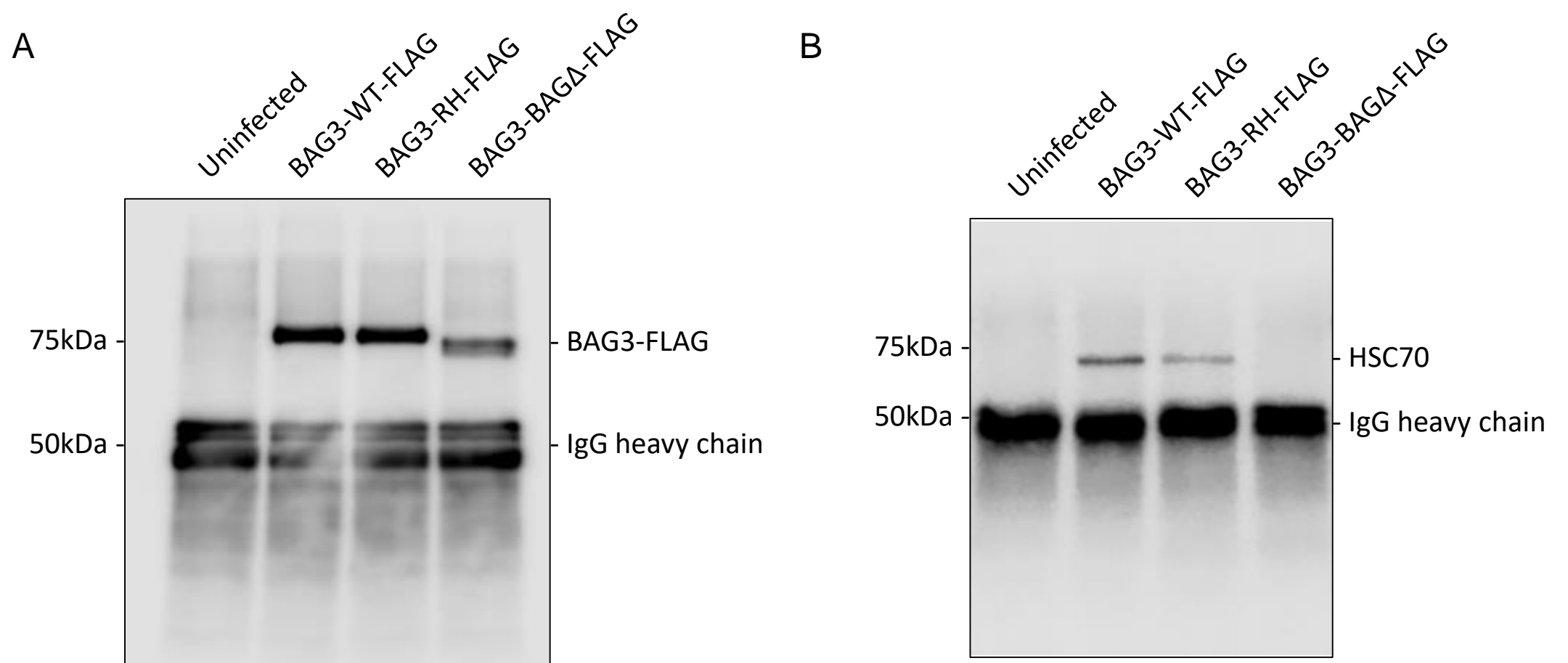


Supplementary Figure 4: MG132-mediated proteasome inhibition activates autophagy and triggers fiber localization of BAG3 in healthy iPSC-derived cardiomyocytes. (A) Western blot analysis of BAG3, P62 and ubiquitinated proteins in iPSC-CMs treated with MG132 (25 μ M) or vehicle alone (DMSO) for 15 hours. (B) Immunocytochemical analysis of BAG3 in control (DMSO) and MG132-treated iPSC-CMs. Green: BAG3, blue: DAPI. Scale bar=20 μ m. Note a mostly cytosolic/diffuse distribution in DMSO-treated cells and a fiber/Z-disc-like distribution in MG132-treated cells. (C) Comparison of BAG3 distribution in iPSC-CMs treated with vehicle (DMSO) alone (n=100) or MG132 (n=176). **P<0.01 Fisher Exact t-test.

Supplementary Figure 5



Supplementary Figure 5: Proteasome inhibition-induced autophagy is dysregulated in BAG3-RH and BAG3-KO iPSC-CMs. (A) Western blot analysis of BAG3-WT, BAG3-RH and BAG3-KO iPSC-CMs following MG132 treatment (25 μ M for 15 hours). (B) Relative abundance of BAG3 (top), ubiquitinated proteins (middle), and LC3-II (bottom) relative to GAPDH based on densitometric analysis of corresponding bands from A.



Supplementary Figure 6: BAG3-HSC70 interaction requires BAG3's BAG domain. (A) Western blot detection of FLAG-tagged BAG3-WT, BAG3-RH and BAG3-BAG Δ following FLAG co-immunoprecipitation of proteins from stably-transduced HL-1 cells. (B) Western blot detection of HSC70 in FLAG co-immunoprecipitates from A.